W

Well-log Analysis of Shale Gas Reservoirs

Reza Rezaee and M. Atif Iqbal
Western Australian School of Mines: Minerals, Energy and Chemical Engineering, Curtin University, Perth, WA, Australia

Definitions

Well-logs provide continuous information about rocks and their pore fluid properties. Typical well-logs such as gamma-ray, density, neutron, sonic, and resistivity logs have been traditionally used to estimate shale volume, porosity, lithology, and fluid saturation in conventional oil and gas exploration, where shale formations are treated as hydrocarbon source rock and sandstone and carbonate formations are reservoir rocks for the migrated oil and gas. However, well-logs interpretation for unconventional shale plays do not follow the same methodologies used for conventional sandstone and carbonate reservoirs. This is due to the complex nature and additional parameters that are required to be estimated for shale reservoirs. Moreover, well-log methodologies for reservoir-fluid characterization have been traditionally advanced and calibrated for sandstone and carbonate rocks. Nevertheless, certain novel concepts and emerging procedures attempt to utilize well-logs for the evaluation of shale reservoirs, including their organic richness, porosities, water saturation, gas volumes, and geomechanical properties.

Introduction

Shale is a very fine-grained, fissile sedimentary rock consisting of mostly clay minerals plus some quartz, carbonates, feldspar, pyrite, and organic matter (OM). Shale or mudstone formations are considered as both hydrocarbon source rock and reservoir rock if they contain sufficient amounts of kerogen (North 1985). Although shale-gas reservoirs show low porosity and permeability, they form laterally widespread and generally thicker formations compared with conventional reservoirs. It is estimated that shale gas could supply more than 7000 trillion cubic feet (tcf) of natural gas reserves globally (Kuuskraa et al. 2013).

To characterize a shale reservoir, several questions need to be addressed. The first question is: How much is the total organic carbon (TOC) of the shale?" The higher organic content indicates a higher quality of shale in terms of gas saturation, porosity, and adsorbed gas content. As a general rule, a shale with less than 2% TOC content cannot be considered a shale gas formation. The next important question: What is the level of thermal maturity of the shale? Clearly, shale gas has to be in the gas generation window. Normally, vitrinite reflectance (R_o) and T_{max} values can be used to answer this question. Positive answers to these two questions indicate the possibility of having a shale gas play in a basin. Other questions that need to be addressed are related to porosity, fluid saturation, and adsorbed gas content that will be used for volumetric calculation of the gas reserves. Brittleness and other geomechanical properties such as Young modulus, Poison's ratio, and rock strength can be used for well-completion and reservoir stimulation purposes. All of these parameters can be estimated from typical well-logs.

The well-log interpretation of shale reservoirs is complicated due to the effect of clays and OM on the logging readings (Iqbal and Rezaee 2020). Typical well-logs consist of gamma-ray (GR), resistivity (R_t), density (RHOB), neutron (NPHI), sonic (DT), and photoelectric factor (PEF). The combination of two or more logs helps to estimate different reservoir properties of shale. This article focuses on the determination of shale reservoir properties using typical well-logs.

The first and fundamental step for the formation evaluation of shale reservoirs is to define a petrophysical model for well-log analysis. Various models have been proposed by different authors (Ambrose et al. 2010; Passey et al. 1990,

R. Sorkhabi (ed.), *Encyclopedia of Petroleum Geoscience*,
https://doi.org/10.1007/978-3-319-02330-4_312-1

2010; Rezaee 2015), one of which is shown in Fig. 1. Shale reservoir rocks consist of the solid matrix and pore space. The solid matrix comprises inorganic and organic matter. Therefore, the porosity can be found as matrix pores and OM pores.

The typical well-logs responses for shale reservoirs can be highlighted as follow:

- High gamma-ray due to radioactive material (clays) and OM in shale formations.
- Mostly high resistivity in shale reservoirs is due to OM and gas content; however, low resistivity can be expected in some cases due to clay content and conductive minerals (e.g., pyrite). The shallow and deep resistivity logs usually overlap due to the lack of drilling fluid invasion.
- Low density due to high OM and gas contents.
- High neutron log response due to clay-bound water (CBW), but decreases with an increase in gas content.
- High sonic log values due to higher OM or gas contents.
- Usually, low PEF log response due to OM.

The major factors that make log responses for shale intervals different from other rock types are the presence of clays with radioactive elements, CBW, and OM in shale. Since the organic richness and the gas content are the major screening factors to identify shale gas intervals, their influences on well-logs can be used to differentiate lean shale from organic-rich or black shale. Organic materials show a density between 1.2 and 1.4 g/cc, whereas inorganic matrix density is mostly between 2.65 and 2.75 g/cc. In general, organic materials, due to their low density, reduce bulk density and increase sonic transit time. The presence of natural gas also reduces bulk density and increases sonic transit time. Both the presence of OM and gas will increase the formation's electrical resistivity. Therefore, any combination of GR, RHOB, DT, and resistivity plots can be used to identify gas shale intervals (Fig. 2).

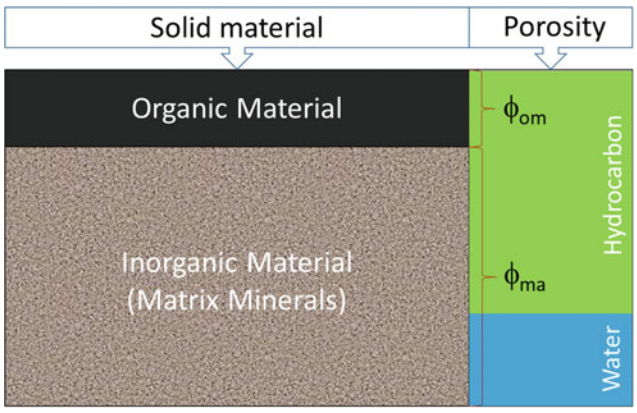

Well-log Analysis of Shale Gas Reservoirs, Fig. 1 A typical petrophysical model for shale gas reservoirs illustrating porosities associated with organic and inorganic materials. (Modified from Iqbal and Rezaee 2020)

Interpretation of Well-Logs

Assessment criteria for shale intervals are completely different from those used to evaluate the conventional hydrocarbon reservoirs. Most of the available data for shale assessment are generally reports on hydrocarbon source rock analysis. These types of information normally were generated during the exploration stage of conventional oil and gas fields. Such reports provide some data about the organic richness of shale (TOC), kerogen type, and thermal maturity using mainly vitrinite reflectance and T_{max}. The other types of available information come from well-logs of drilled boreholes. There have been many attempts to use typical well-logs to estimate shale characteristics such as TOC, R_o, porosity, fluid saturation, and the brittleness (e.g., Schmoker and Hester 1983; Passey et al. 1990; Rickman et al. 2008; Sondergeld et al. 2010; Rezaee 2015; Kadkhodaie and Rezaee 2016; Testamanti and Rezaee 2017). In the following sections, common methods to estimate shale reservoir properties from well-logs are briefly discussed.

TOC Estimation

Modern logging tools that use the same concept of neutron-induced captured gamma-ray utilized in the old tools directly measure carbon content (Gonzalez et al. 2013). These geochemical logging tools can be used for TOC estimation. For example, the pulsed neutron spectrometry (PNS) tool measures the total carbon amount for any rock formation ($C_{measured}$). The measured total carbon includes carbon in carbonate minerals (e.g., calcite, dolomite, or siderite) as well as organic carbon (C_{TOC}). Therefore, the difference between the total or measured carbon in the formation and carbon in carbonates provides the TOC content (Jacobi et al. 2009) as shown in the following relationship (Eq. 1):

$$C_{TOC} = C_{measured} - (C_{calcite} + C_{dolomite} + C_{siderite}) \quad (1)$$

The elemental ratio of silicon to carbon is then used to determine whether excess carbon from coal is present or not. The difference between carbon in oil or OM can be estimated based on a cut-off value for uranium. If uranium is more than the minimum value, then the excess carbon is OM; otherwise, it would be from hydrocarbon. The proposed cut-off value for uranium is from 4 to 7 ppm (Pemper et al. 2009).

The above example can, however, be rarely used for shale gas studies in the majority of boreholes due to the scarcity of advanced well-log data. However, many published papers

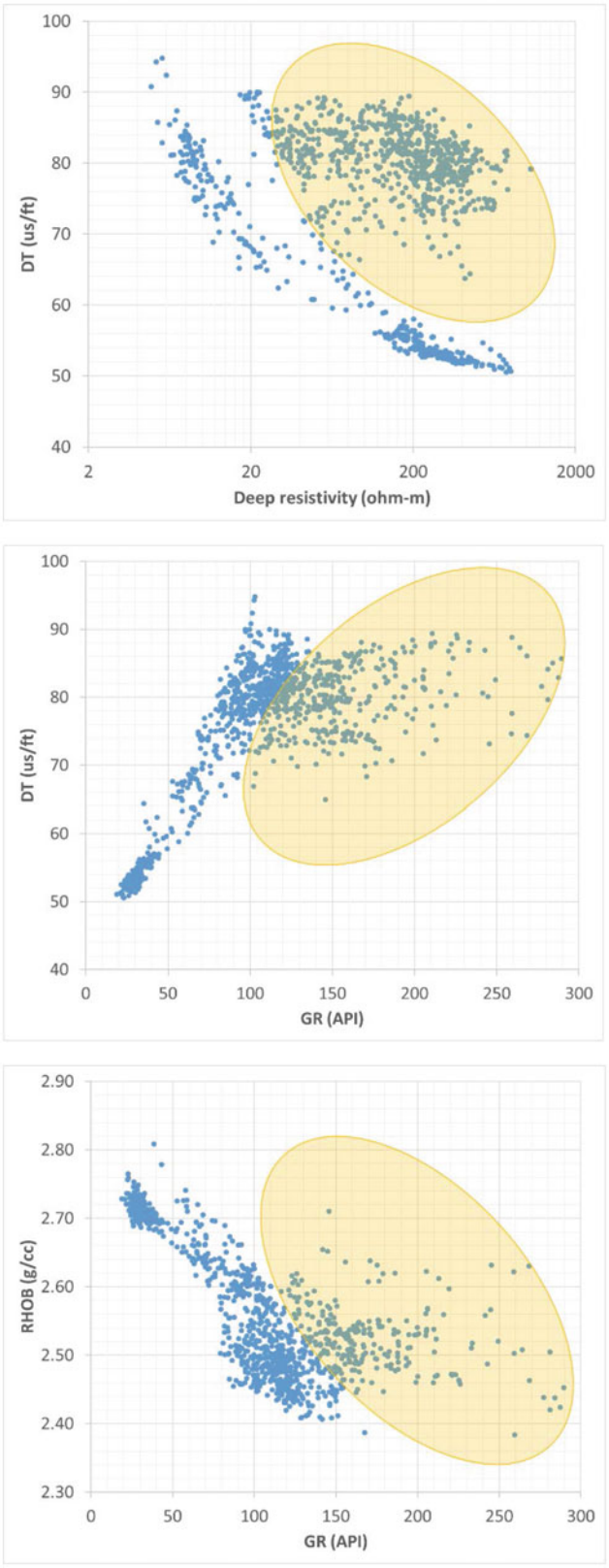

Well-log Analysis of Shale Gas Reservoirs, Fig. 2 Examples of deep resistivity, sonic (DT), gamma-ray (GR), and bulk density (RHOB) cross plots to differentiate shale gas from other lithologies in the Barnett Shale. Highlighted enclosed data points in all three graphs are productive shale gas intervals

have used typical well-logs for TOC estimation. One of the most widely used approaches for TOC calculation is the Passey method (Passey et al. 1990). This method overlaps a scaled porosity log (mainly sonic transit time curve) on a deep resistivity log. The separation between sonic and deep resistivity logs can be defined by the baselines (Eq. 2):

$$\Delta \log R = \log_{10}\left(\frac{R}{R_{baseline}}\right) + 0.02 \times (\Delta t - \Delta t_{baseline}) \quad (2)$$

where ΔlogR is the separation between deep resistivity and sonic logs, R and Δt are deep resistivity and sonic transit time respectively, and $R_{baseline}$ and $\Delta t_{baseline}$ are respectively unique baseline values of resistivity and sonic transit time for a lean shale. Then, TOC can be determined by the following equation (Eq. 3):

$$TOC = \Delta \log R \times 10^{2.297 - 0.1688 \times LOM} \quad (3)$$

where the level of organic maturity (LOM) can be determined by the relationship of TOC and S_2 from pyrolysis tests as proposed by Passey et al. (1990) or from vitrine reflectance (R_o) data (Alshakhs and Rezaee 2017; Johnson 2019). Although this method is scientifically sound, its major withdraw is the difficulty of getting correct baseline values for a lean shale interval and correct values for LOM. Within a borehole, a lean or barren shale could have completely different compositional and petrophysical properties from an organic-rich shale, thus making this approach uncertain in some cases.

Considering fluctuations in the bulk density (RHOB) due to the presence or absence of OM, an empirical relationship was developed (Schmoker and Hester 1983) to estimate TOC in shales. The following equation (Eq. 4) is defined as the Schmoker method:

$$TOC\ (wt\%) = \frac{154.497}{RHOB} - 57.261 \quad (4)$$

The constants in the equation were calculated explicitly for the upper and lower shale members of the Bakken Formation by maintaining OM density as 1.01 g/cc and matrix density as 2.68 g/cc. This means that the equation is applicable for shale formations with the same levels of OM and matrix densities.

In principle, a linear correlation between measured TOC and density log can provide a reliable equation for TOC estimation in shale formations. However, comprehensive log data quality control and detailed depth matching between core and log data are essential for such an approach.

Vernik and Landis (1996) introduced an empirical relationship for TOC estimation from density log (Eq. 5):

$$\mathrm{TOC}\ (\mathrm{wt}\%) = 67 \times \frac{\mathrm{RHO_k}(\mathrm{RHO_m} - \mathrm{RHO_s})}{\mathrm{RHO_s}(\mathrm{RHO_m} - \mathrm{RHO_k})} \quad (5)$$

Where, $\mathrm{RHO_k}$ is kerogen density, $\mathrm{RHO_m}$ is matrix density, and $\mathrm{RHO_s}$ is grain density (from core data).

This method requires analytical information from core and cuttings, such as grain density, thus limiting its use when there is no core analysis data available.

The bulk density of a shale interval could be controlled by several factors including burial depth, mineralogical composition, and TOC content. Therefore, to introduce a universal equation, all these parameters need to be considered. Alshakhs and Rezaee (2017) proposed the following linear relationship (Eq. 6) that somehow considers shale composition and burial depth from GR and DT log inputs. Note, however, that the presence of pyrite and other heavy minerals may result in the underestimation of TOC for these types of equations.

$$\mathrm{TOC} = 0.0195\mathrm{GR} + 0.12\mathrm{DT} - 0.3\mathrm{RHOB} - 8.24 \quad (6)$$

where GR is the gamma-ray log, DT is sonic transit time (us/ft), and RHOB is bulk density log reading (g/cc).

Several papers have used machine learning methods using well-log inputs to estimate TOC (Kadkhodaie-Ilkhchi et al. 2009; Khoshnoodkia et al. 2011; Ouadfeul and Aliouane 2014; Tan et al. 2015; Yu et al. 2016).

Porosity Determination

Porosity logging tools, such as density, sonic, and neutron, must be used with caution for porosity estimation in shale reservoirs. The presence of OM and gas can affect log readings, thus rendering the common porosity-log relations problematic for shales. For example, the following simple relation of density and porosity (Eq. 7) will not work for shales, and only works for conventional clean reservoirs (e.g., clean sandstone):

$$\rho b = Ø\rho_f + (1 - Ø)\rho_{ma}$$

$$ØD = \frac{\rho_{ma} - \rho_b}{\rho_{ma} - \rho_f} \quad (7)$$

However, for shale reservoirs, kerogen content needs to be considered in the above relation (Eq. 8).

$$\rho_b = Ø\rho_f + (1 - Ø - V_k)\rho_{ma} + V_k\rho_k \quad (8)$$

where ρ_b is bulk density (g/cc), $Ø_D$ *is* density porosity (v/v), ρ_{ma} is matrix density (g/cc), ρ_f is fluid density (g/cc), V_k is the kerogen volume (v/v), and ρ_k is kerogen density (g/cc).

Several authors have proposed corrections of the porosity logs based on kerogen volume (Iqbal and Rezaee 2020; Sondergeld et al. 2010; Yu et al. 2018). The following equation (Eq. 9) proposed by Iqbal and Rezaee (2020) and Yu et al. (2018) can be used for porosity estimation in shale reservoirs using density log:

$$ØD_{\mathrm{Total}} = \left[\left(\frac{\rho_{ma} - \left(\frac{\rho_b - \rho_k \times V_k}{1 - V_k}\right)}{\rho_{ma} - \rho_f}\right) + (0.2 \times \mathrm{TOC} * \rho_b)\right] \quad (9)$$

Since the organic content of shales from well-logs is generally estimated as weight fraction, it must be converted to volume fraction (Eq. 10):

$$V_k = \frac{\mathrm{KC} * \mathrm{TOC} * \rho_b}{\rho_k} \quad (10)$$

where KC is the kerogen conversion factor determined from kerogen types (Table 1) or considered to be 1.19 for most shale gas reservoirs in case there is no independent information about kerogen type.

The kerogen density can be determined by Eqs. 11 or 12 introduced by Iqbal and Rezaee (2020); Ward (2010):

$$\rho_k = 0.342 \times R_O + 0.972 \quad (11)$$

$$\frac{1}{\rho_{\mathrm{grain}}} = A \times \mathrm{TOC} + B \quad (12)$$

where R_O is the vitrinite reflectance and ρ_{grain} is considered as the matrix density when TOC content is zero. A and B are constants derived from the linear relationship obtained in Fig. 3. The relationship illustrated in Fig. 3 shows that the matrix density of samples in that study is 2.79 g/cc (the intercept of regression line at zero percentage of TOC), and kerogen density is 1.24 g/cc (when TOC is 100%) (Iqbal and Rezaee 2020).

The porosity can also be determined by the following equation (Eq. 13) based on sonic logs proposed by Rezaee (2015):

Well-log Analysis of Shale Gas Reservoirs, Table 1 TOC to kerogen conversion factor proposed by Tissot and Welte (1984)

	Type of kerogen		
Stage	I	II	III
Diagenesis	1.25	1.34	1.48
End of catagenesis	1.20	1.19	1.18

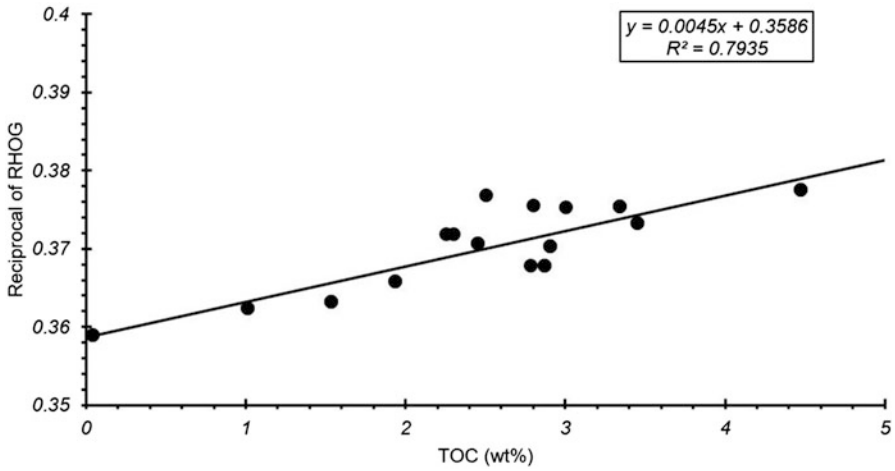

Well-log Analysis of Shale Gas Reservoirs, Fig. 3 Kerogen and matrix densities determination in shales based on an empirical relationship between core-based TOC and reciprocal grain density (Iqbal and Rezaee 2020)

$$Ø_{sonic} = \frac{(DT - DT_{ma}) + \left(\frac{w_{TOC}}{\rho_k} \times \rho_b\right) \times (DT_{ma} - DT_k)}{DT_f - DT_{ma}} \quad (13)$$

where DT is rock transit time (μsec/ft); DT_{ma} is matrix transit time (μsec/ft); w_{TOC} is total organic carbon content weight (wt%); DT_k is kerogen transit time (μsec/ft), which for coal is recorded as 120 μsec/ft.; and DT_f is fluid transit time (μsec/ft).

The porosity calculated from the above equations is total porosity that considers CBW part of the pore space. To exclude CBW volume and thus to calculate effective porosity, Yuan and Rezaee (2019) introduced a relationship (Eq. 14) to calculate CBW based on shale volume (V_{sh}) for illite-rich shales:

$$CBW(\%) = 0.19 \times V_{sh}(\%) - 0.7 \quad (14)$$

Therefore, effective porosity can be calculated by subtracting CBW from the total porosity obtained from Eq. 9 or Eq. 13.

Water Saturation (S_w) Calculation

Water saturation determination is relatively straight-forward for the clean conventional reservoirs by using Archie's equation (Eq. 15) (Archie 1942):

$$S_w = \sqrt[n]{\frac{a.R_w}{\phi^m.R_t}} \quad (15)$$

where R_t is true formation resistivity (ohm-m), Ø is porosity (v/v), m is cementation exponent, n is saturation exponent usually equals to 2, a is tortuosity factor usually taken as 1, and R_w is formation water resistivity (ohm-m). This equation works well for clean reservoir rocks. For shaly sand formations, due to excessive conductivity exerted by clays, the Archie equation was modified, and several equations were introduced. Excessive conductivity was considered either by V_{sh} or the cation exchange capacity (CEC) concepts. Simandoux (1963) utilized the V_{sh} method, which is widely used for shaly reservoirs (Eq. 16):

$$S_w = \frac{aR_W}{2\phi^m}\left[-\frac{V_{sh}}{R_{sh}} + \left(\left(\frac{V_{sh}}{R_{sh}}\right)^2 + \frac{4\phi^m}{aR_WR_t}\right)^{0.5}\right] \quad (16)$$

where R_{sh} is shale resistivity (ohm-m) and V_{sh} is shale volume (fraction).

All of the proposed equations for shaly sand formations are based on the conductivities of clay and nonclay matrix only. Therefore, these models overestimate the water saturation in shale reservoirs and do not provide a correct S_w.

A simple Archie equation, that has long been used for quick S_w calculation for clean formations, was introduced by Labani and Rezaee (2015) to calculate S_w for shales (Eq. 17):

$$S_w = \sqrt[n]{\frac{R_o}{R_t}} \quad (17)$$

where R_o is the deep resistivity in lean shale interval (ohm-m) and R_t is the deep resistivity log reading in the organic-rich shale (ohm-m). This approach is a quick way of S_w calculation for shale reservoirs and does not require unknown or complex inputs. For detailed calculations of S_w by the modified Archie equation, refer to Iqbal and Rezaee (2020) and Kadkhodaie and Rezaee (2016). Due to the presence of clay minerals and OM in shale, it is crucial to apply the necessary corrections to obtain the true resistivity (R_t) from the logging readings. It is well known that the clay minerals reduce the formation resistivity and the OM enhances the resistivity. Therefore, the TOC and V_{sh} corrections can be used for R_t

using the equation proposed by Iqbal and Rezaee (2020) (Eq. 18):

$$S_w = \sqrt{\frac{F * Rw}{R_t - \left(TOC^2 * R_{TOC}\right) + \left(V_{sh}^2 * R_{sh}\right)}} \quad (18)$$

A simpler equation can be presented in the form of Eq. 19:

$$S_w = \sqrt{\frac{R_0}{R_t - \left(TOC^2 * R_{TOC}\right)}} \quad (19)$$

where R_0 is the rock resistivity in lean shale interval where water saturation is deemed 100%, R_t is true resistivity of organic-rich shale formation, TOC is total organic carbon content (fraction), and R_{TOC} is organic material resistivity. R_{TOC} can be determined by establishing a relationship between true log resistivity and TOC as developed by Iqbal and Rezaee (2020) and given below as Eq. 20. In Fig. 4 where TOC is 100%, R_t could be considered equal to R_{TOC} which is about 611.6 ohm-m for this case.

$$R_{TOC}(\text{ohm} - \text{m}) = \frac{TOC\ (\text{wt}\%)}{0.1635} = \frac{100}{0.1635} = 611.6 \quad (20)$$

Volumetric Calculation of Stored Gas

In shale gas reservoirs, natural gas is stored as free gas, inside the pore spaces of the rock, and as adsorbed gas, mostly on the surface of the organic material. The volumes of these two types of gas accumulations need to be calculated separately. Total gas, which is the summation of free gas and adsorbed gas, can then be used for the volumetric calculation of a shale gas reservoir.

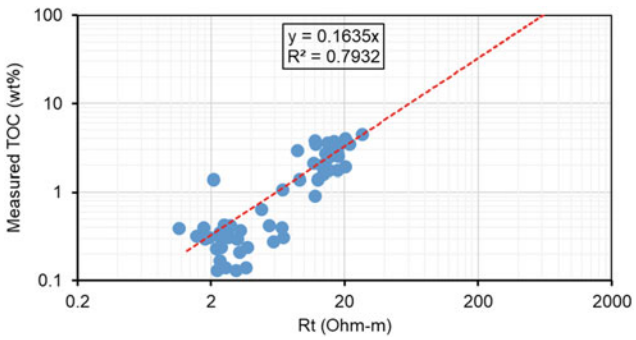

Well-log Analysis of Shale Gas Reservoirs, Fig. 4 Relationship between true resistivity and measured total organic carbon (modified from Iqbal and Rezaee 2020) for Goldwyer Shale, Canning Basin, Western Australia

After determination of porosity and water saturation, the original gas in place for free gas (in pore spaces) can be estimated by applying the following general volumetric equation (Eq. 21):

$$gc_{Free} = \frac{A \times h \times \phi \times (1 - S_w)}{B_g} \quad (21)$$

where gc_{Free} is free gas content, A is reservoir area, h is reservoir thickness, ϕ is effective porosity, S_w is water saturation, and B_g is gas formation volume factor. Under normal pressure conditions, B_g can be approximated by the following equation (Eq. 22):

$$B_g = 11.25/\text{depth (in meter)} \quad (22)$$

The gas adsorption capacity of shale is usually determined by a high-pressure methane adsorption test on shale samples or through a desorption test for fresh samples (Ekundayo and Rezaee 2019; Gou et al. 2020; Jia et al. 2018; Sudibandriyo et al. 2003). However, different researchers have introduced some established relationships that can be used to estimate the adsorbed gas content through well-log analysis (Gou et al. 2020; Zou and Rezaee 2019).

In general, the Langmuir model is used to predict the methane adsorption at specific reservoir pressure and temperature (Eq. 23):

$$g_c(T) = \frac{V_L(T) \times P}{P_L(T) + P} \quad (23)$$

where $g_c(T)$ is the adsorbed gas content at a specific temperature (scf/ton), $V_L(T)$ is the Langmuir volume at reservoir temperature (scf/ton), $P_L(T)$ is the Langmuir pressure at reservoir temperature (psi), and P is the reservoir pore pressure (psi). It can be observed that $V_L(T)$ and $P_L(T)$ are the main parameters in the above equation to be used for the determination of adsorbed gas content. These parameters can be predicted by the following equations (Eqs. 24 and 25) proposed by Zou and Rezaee (2019):

$$V_L(T) = (13.87TOC + 0.79V_{sh} - 4) - (T - T_O)(0.35TOC - 0.05) \quad (24)$$

$$P_L(T) = 93.8 \ln(13.87TOC + 0.79V_{sh} - 13.3) \times e^{\left(1215.3TOC^{0.179}\right)} \times \left(\frac{1}{T_o + 273} - \frac{1}{T + 273}\right) \quad (25)$$

where $V_L(T)$ is the Langmuir volume at reservoir temperature (scf/ton), TOC is total organic carbon content (wt%), V_{sh} is the volume of shale can be determined by gamma-ray log (%),

T is the reservoir temperature that can be estimated by the temperature gradient (°C), T_O is the experimental temperature (°C) which is normally around 25 °C, and $P_L(T)$ is the Langmuir pressure at reservoir temperature (psi).

The adsorbed gas in place ($GIP_{adsorbed}$) can be obtained by the following equation (Eq. 26):

$$GIP_{adsorbed} = g_c(T) \times \rho_b \times A \times h \tag{26}$$

where $g_c(T)$ is the adsorbed gas content at a specific temperature and pressure (scf/ton), ρ_b is bulk density (g/cc) of the rock, A is reservoir area, and h is reservoir thickness.

Brittleness Index Determination

The brittleness index is helpful to understand the capability of any shale to be fractured through the hydraulic fracturing process. It can be determined using various equations proposed by different authors, based on mineral composition and geomechanical properties (e.g., Young's modulus E and Poisson's ration v).

Rickman et al. (2008) and Grieser and Bray (2007) introduced brittleness index determination through the combination of Young's modulus E and Poisson's ratio v. These two parameters are combined to determine the rock strength to be failed under stress in terms of Poisson's ratio and how the rock can maintain a fracture (Young's modulus). The interdependence of these two parameters and their relationship with the brittleness index are illustrated in Fig. 5, indicating that a brittle shale should have a higher Young's modulus and lower Poisson's ratio.

The dynamic Young's modulus and Poisson's ratio can be calculated using the log data of compressional and shear velocities according to the following Eq. 27:

$$E_{dyn} = \frac{\rho V_s^2\left(3V_p^2 - 4V_s^2\right)}{V_p^2 - V_s^2} \tag{27}$$

where E_{dyn} is dynamic Young's modulus, ρ is the bulk density, and Vp and Vs are compressional and shear wave velocities, respectively.

There are many relationships established by different authors to express static Young's modulus (E_{sta}) in terms of dynamic Young's modulus; one of them was introduced by Mandal et al. (2020) as follows (Eq. 28):

$$E_{sta} = 0.705 \times E_{dyn} - 6.8935 \tag{28}$$

In the same way, the dynamic (v_{dyn}) and static (v_{sta}) Poisson's ratios can be determined using Eqs. 29 and 30:

$$v_{dyn} = \frac{V_p^2 - 2V_s^2}{2\left(V_p^2 - V_s^2\right)} \tag{29}$$

$$v_{sta} = 0.8 \times v_{dyn} - 6.8935 \tag{30}$$

After the determination of Young's modulus and Poisson's

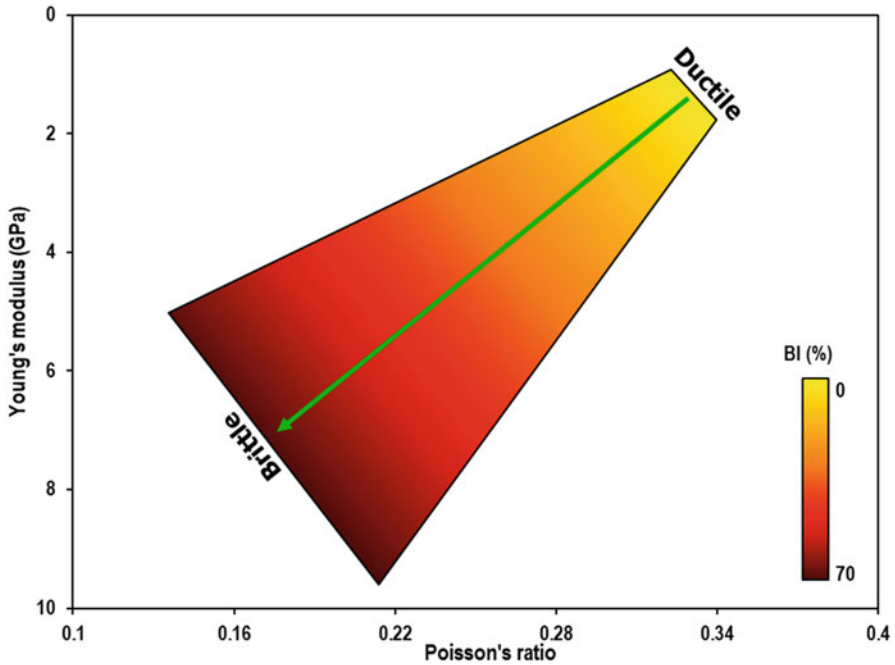

Well-log Analysis of Shale Gas Reservoirs, Fig. 5 A cross-plot illustrating the rock brittleness based on the Poisson's ratio and Young's modulus, modified from Rickman et al. (2008)

ratio, these parameters can be normalized by using the following equations (Eqs. 31 and 32):

$$E_{brittle} = \frac{E - E_{min}}{E_{max} - E_{min}} \quad (31)$$

$$v_{brittle} = \frac{v - v_{min}}{v_{max} - v_{min}} \quad (32)$$

Finally, the brittleness index can be determined according to Eq. 33:

$$BI_{sonic} = \frac{E_{brittle} + v_{brittle}}{2} \times 100 \quad (33)$$

It can be observed that the full-waveform sonic data (shear wave and compressional wave velocities) are required to estimate rock elastic parameters. However, sometimes, shear velocity data is not available, in which case the following empirical formula proposed by Castagna et al. (1985) can be used (Eq. 34):

$$V_s = 0.862 \times V_p - 1.172 \quad (34)$$

Vp and Vs in Eq. 34 are in km/s and can directly be calculated from DT (us/ft) by the following conversions:

$$Vp\ (km/s) = 304.8/DTc\ (us/ft) \quad (35)$$

Estimation of Unconfined Compressive Strength

Unconfined (uniaxial) compressive strength (UCS) of a rock is a common measure of the strength of intact rock and the widely used test performed for boreability prediction and geomechanical consideration for optimization of a hydraulic fracturing design. It is normally measured on cylinders of rock core by compressing the core and measuring the maximum load at which the rock failure occurs. UCS is calculated by dividing the maximum load at the failure by the sample cross-sectional area. Khaksar et al. (2009) reviewed 44 empirical equations introduced for the unconfined compressive strength estimation. In most of these empirical equations for estimation of rock strength from wireline logs, three main inputs included elastic wave velocity, Young's modulus, and porosity. Elastic wave velocity, especially Vp, can be derived from sonic transit time, and Young's modulus can be calculated from sonic velocity and density logs. Porosity can also be determined by porosity logs such as density and neutron. Of the equations proposed to calculate the UCS for shale formations, one of them that directly utilized sonic log data is by Horsrud (2001) introduced for shales from the North Sea (Eq. 36).

$$UCS\ (MPa) = 0.77V_p^{2.93} \quad (36)$$

Where Vp is compressional wave velocity in km/s.

Summary

Well-log analysis based on a combination of typical logs such as gamma-ray (GR), resistivity (R_t), density (RHOB), neutron (NPHI), sonic (DT), and photoelectric factor (PEF) is helpful to obtain continuous information about petrophysical and geomechanical properties of shale reservoirs and their fluids. This information is beneficial to identify sweet spots in shale plays. However, this field is in its infancy, and a great deal needs to be done to advance and calibrate the concepts and methodologies of well logs traditionally applied to sandstone and carbonate reservoirs. Problems in well-log interpretation of shale reservoirs arise from the very tight nature of these rocks, the presence of OM and inorganic minerals (especially clay minerals), as well as our poor knowledge of shale porosities and hydrocarbon saturation – critical attributes to be estimated from well-log readings. Based on the current knowledge, this entry briefly reviewed various quantitative methodologies for estimation of total organic carbon (TOC), porosities, water saturation, and volumes of free and adsorbed gas in shale formation. Moreover, since shale formations are hydraulically fractured for hydrocarbon recovery, the brittle index of shale was also discussed from a geomechanical viewpoint.

Cross-References

- ▶ Mudrocks
- ▶ Petrographic Imaging Methods for Characterizing Mudstone Reservoirs
- ▶ Production of Liquid Hydrocarbons from Shale
- ▶ Storage Mechanisms of Oil and Gas in Shale
- ▶ Tight Oil

Nomenclature

ΔlogR	Separation between deep resistivity and sonic logs
Δt	TRansit time from the sonic log (μsec/ft)
ØD	Density porosity
ρ_{ma}	Matrix density
ρ_b	Bulk density (g/cc)
ρ_f	Fluid density
KC	Kerogen conversion factor
ρ_k	Kerogen density (g/cc).

ρ_{grain}	Grain density
ρ_{bk}	Kerogen corrected bulk density
Ø	Porosity
Øk	Kerogen porosity
$ØD_{Total}$	Total density porosity
a	Tortuosity factor
BI	Brittleness index
Cc	Convertible carbon fraction
C_t	Total conductivity
C_w	Formation water conductivity
DT	Rock transit time (μsec/ft)
DT_f	Fluid transit time(μsec/ft)
DT_k	Kerogen transit time (μsec/ft)
DT_{ma}	Matrix transit time (μsec/ft)
E_{dyn}	Dynamic Young's modulus
E_{sta}	Static Young's modulus
$g_c(T)$	Adsorbed gas content at specific temperature and pressure (scf/ton)
HIp	Present hydrogen index
HIo	Original hydrogen index
LOM	Level of organic maturity
m	Cementation exponent
n	Saturation exponent
PIp	Present production index
PIo	Original production index
P	Reservoir pore pressure (psi)
P_G	Formation pressure coefficient
$P_L(T)$	Langmuir pressure at reservoir temperature (psi)
RHO_k	Kerogen density
RHO_s	Grain density
R_w	Formation water resistivity
R_{sh}	Resistivity of shale
R_t	True resistivity in ohm-m
R_o	The rock resistivity in lean shale interval where water saturation is deemed 100%
R_{TOC}	Organic material resistivity
S_w	Water saturation
SCF	Standard cubic feet
TOC	Total organic carbon content
TOCo	Original total organic carbon
TR	Transformation ratio
V_k	Kerogen volume in fractions
Vp	Compressional wave velocity
Vs	Shear wave velocity
$V_L(T)$	Langmuir volume at reservoir temperature (scf/ton)
V_{sh}	Volume of shale
w_{TOC}	Total organic carbon content weight (wt%)

Bibliography

Alshakhs M, Rezaee MR (2017) A new method to estimate total organic carbon (TOC) content: an example from goldwyer shale formation, the Canning Basin. Open Petroleum Eng J 10:118–133

Ambrose RJ, Hartman RC, Diaz Campos M, Akkutlu IY, Sondergeld C (2010) New pore-scale considerations for shale gas in place calculations. SPE unconventional gas conference, Pittsburgh, February 2010. https://doi.org/10.2118/131772-MS

Archie GE (1942) The electrical resistivity log as an aid in determining some reservoir characteristics. AIME Trans 146(01):54–62

Castagna JP, Batzle ML, Eastwood RL (1985) Relationships between compressional-wave and shear-wave velocities in clastic silicate rocks. Geophysics 50(4):571–581

Ekundayo JM, Rezaee R (2019) Effect of equation of states on high-pressure volumetric measurements of methane–coal sorption isotherms – part 1: volumes of free space and methane adsorption isotherms. Energy Fuel 33(2):1029–1036

Gonzalez J, Lewis R, Hemingway J, Grau J, Rylander E, Pirie I (2013) Determination of formation organic carbon content using a new neutron-induced gamma ray spectroscopy service that directly measures carbon. Unconventional Resources Technology Conference, Denver, 12–14 Aug 2013. https://doi.org/10.1190/urtec2013-112

Gou Q, Xu S, Hao F, Zhang B, Shu Z, Yang F, Wang Y, Li Q (2020) Quantitative calculated shale gas contents with different lithofacies: a case study of Fuling gas shale, Sichuan Basin, China. J Nat Gas Sci Eng 76:103222

Grieser WV, Bray JM (2007) Identification of production potential in unconventional reservoirs. Production and Operations Symposium, Oklahoma City, March 2007. https://doi.org/10.2118/106623-MS

Horsrud P (2001) Estimating mechanical properties of shale from empirical correlations. SPE Drill Complet 16(02):68–73

Iqbal MA, Rezaee R (2020) Porosity and water saturation estimation for shale reservoirs: an example from goldwyer formation shale, Canning Basin, Western Australia. Energies 13(23):62–94

Jacobi DJ, Breig JJ, LeCompte B, Kopal M, Hursan G, Mendez FE, Bliven S, Longo J (2009) Effective geochemical and geomechanical characterization of shale gas reservoirs from the wellbore environment: caney and the Woodford shale. SPE annual technical conference & exhibition, New Orleans, Oct 2009. https://doi.org/10.2118/124231-MS

Jia B, Tsau J-S, Barati R (2018) Different flow behaviors of low-pressure and high-pressure carbon dioxide in shales. SPE J 23(04): 1,452–451,468

Johnson LM (2019) Integrated reservoir characterization of the goldwyer formation, Canning Basin. Curtin University, WASM: Minerals, Energy and Chemical Engineering, PhD thesis, http://hdl.handle.net/20.500.11937/77189

Kadkhodaie A, Rezaee R (2016) A new correlation for water saturation calculation in gas shale reservoirs based on compensation of kerogen-clay conductivity. J Pet Sci Eng 146:932–939. https://doi.org/10.1016/j.petrol.2016.08.004

Kadkhodaie-Ilkhchi A, Rahimpour-Bonab H, Rezaee M (2009) A committee machine with intelligent systems for estimation of total organic carbon content from petrophysical data: an example from Kangan and Dalan reservoirs in South Pars Gas Field, Iran. Comput Geosci 35(3):459–474

Khaksar A, Taylor PG, Fang Z, Kayes TJ, Salazar A, Rahman K (2009) Rock strength from core and logs, where we stand and ways to go. EUROPEC/EAGE Conference & Exhibition, Amsterdam, June 2009. https://doi.org/10.2118/121972-MS

Khoshnoodkia M, Mohseni H, Rahmani O, Mohammadi A (2011) TOC determination of Gadvan Formation in South Pars Gas field, using artificial intelligent systems and geochemical data. J Pet Sci Eng 78(1):119–130

Kuuskraa V, Stevens SH, Moodhe KD (2013) Technically recoverable shale oil and shale gas resources: an assessment of 137 shale formations in 41 countries outside the United States. US Energy Information Administration, US Department of Energy, Washington, DC

Labani M, Rezaee R (2015) Petrophysical evaluation of gas shale reservoirs. In: Rezaee R (ed) Fundamentals of gas shale reservoirs. Wiley, New York, pp 114–134

Mandal PP, Sarout J, Rezaee R (2020) Geomechanical appraisal and prospectivity analysis of the Goldwyer shale accounting for stress variation and formation anisotropy. Int J Rock Mech Min Sci 135: 104513

North F (1985) Petroleum geology. Allen amp Unwin, Boston, pp 253–341

Ouadfeul S-A, Aliouane L (2014) Shale gas reservoirs characterization using neural network. Energy Procedia 59:16–21

Passey Q, Creane S, Kulla J, Moretti F, Stroud J (1990) A practical model for organic richness from porosity and resistivity logs. AAPG Bull 74(12):1777–1794

Passey QR, Bohacs K, Esch WL, Klimentidis R, Sinha S (2010) From oil-prone source rock to gas-producing shale reservoir-geologic and petrophysical characterization of unconventional shale gas reservoirs. International Oil and Gas Conference & Exhibition in China, Beijing, SPE-131350-MS. https://doi.org/10.2118/131350-MS

Pemper RR, Han X, Mendez FE, Jacobi D, LeCompte B, Bratovich M, Feuerbacher G, Bruner M, Bliven S (2009) The direct measurement of carbon in wells containing oil and natural gas using a pulsed neutron mineralogy tool. SPE annual technical conference & exhibition, New Orleans, Oct 2009. Paper Number: SPE-124234-MS. https://doi.org/10.2118/124234-MS

Rezaee R (ed) (2015) Fundamentals of gas shale reservoirs. Wiley, New York

Rickman R, Mullen MJ, Petre JE, Grieser WV, Kundert D (2008) A practical use of shale petrophysics for stimulation design optimization: all shale plays are not clones of the Barnett Shale. SPE annual technical conference & exhibition, Denver, Sept 2008.; Paper Number: SPE-115258-MS. https://doi.org/10.2118/115258-MS

Schmoker JW, Hester TC (1983) Organic carbon in Bakken formation, United States portion of Williston basin. AAPG Bull 67(12): 2165–2174

Simandoux P (1963) Dielectric measurements in porous media and application to shaly formation. Revue del'Institut Francais du Petrole 18(Suppl Issue):193–215

Sondergeld CH, Newsham KE, Comisky JT, Rice MC, Rai CS (2010) Petrophysical Considerations in Evaluating and Producing Shale Gas Resources. SPE Unconventional Gas Conference, Pittsburgh, Pennsylvania; Paper Number: SPE-131768-MS. https://doi.org/10.2118/131768-MS

Sudibandriyo M, Pan Z, Fitzgerald JE, Robinson RL, Gasem KA (2003) Adsorption of methane, nitrogen, carbon dioxide, and their binary mixtures on dry activated carbon at 318.2 K and pressures up to 13.6 MPa. Langmuir 19(13):5323–5331

Tan M, Song X, Yang X, Wu Q (2015) Support-vector-regression machine technology for total organic carbon content prediction from wireline logs in organic shale: a comparative study. J Nat Gas Sci Eng 26:792–802

Testamanti MN, Rezaee R, Zou J (2017). Porosity and Pore Size Distribution of Shales: A Case Study of the Carynginia Formation, Perth Basin, Western Australia. Extended abstract, The APPEA Journal 57: 660–663. Presented at the APPEA Annual Conference and Exhibition, May 14–17, 2017, Perth, Western Australia

Tissot BP, Welte DH (1984) Petroleum formation and occurrence, 2nd edn. Springer, pp 69–73

Ward J (2010) Kerogen density in the Marcellus Shale. SPE Unconventional Gas Conference, Pennsylvania, Paper Number: SPE-131767-MS. https://doi.org/10.2118/131767-MS

Yu H, Wang Z, Rezaee R, Zhang Y, Xiao L, Luo X, Wang X, Zhang L (2016) The gaussian process regression for TOC Estimation using wireline logs in shale gas reservoirs. International Petroleum Technology Conference, Bangkok, Thailand, Paper Number: IPTC-18636-MS. https://doi.org/10.2523/IPTC-18636-MS

Yu H, Wang Z, Rezaee R, Zhang Y, Han T, Arif M, Johnson L (2018) Porosity estimation in kerogen-bearing shale gas reservoirs. J Nat Gas Sci Eng 52:575–581. https://doi.org/10.1016/j.jngse.2018.02.012

Yuan Y, Rezaee R (2019) Comparative porosity and pore structure assessment in shales: measurement techniques, influencing factors and implications for reservoir characterization. Energies 12(11):2094

Zou J, Rezaee R (2019) A prediction model for methane adsorption capacity in shale gas reservoirs. Energies 12(2):280